Increasing the size of rAAV-mediated expression cassettes in vivo by intermolecular joining of two complementary vectors

Hiroyuki Nakai, Theresa A. Storm, and Mark A. Kay*

*Program in Human Gene Therapy, Department of Pediatrics and Genetics, Stanford University, Stanford, CA 94305. *Corresponding author (markay@stanford.edu).*

Received 6 January 2000; accepted 20 March 2000

A major shortcoming to the use of adeno-associated virus (rAAV) vectors is their limited packaging size. To overcome this hurdle, we split an expression cassette and cloned it into two separate vectors. The vectors contained either a *nuclear localizing Escherichia coli lacZ* transgene (*nlslacZ*) with a splice acceptor, or the *human elongation factor 1*α (*EF1*α) gene enhancer/promoter(s) (EF1αEP) with a splice donor. We co-injected a promoter-less *nlslacZ* vector with a vector containing either a single EF1αEP or a double copy of the EF1αEP in a head-to-head orientation, into the portal vein of mice. Gene expression, measured by both transduction efficiency and quantitation of the recombinant protein, was as much as 60–70% of that obtained from mice that received a single vector containing a complete EF1αEP/nlslacZ expression cassette. This two-vector approach may allow development of gene therapy strategies that will carry exogenous DNA sequences with large therapeutic cDNAs and/or regulatory elements.

Keywords: adeno-associated virus vector, gene therapy, hepatocytes, intermolecular recombination, concatemer

Recombinant adeno-associated virus (rAAV) vectors based on AAV type 2 can safely transduce various tissues and result in persistent gene expression in vivo[1–7]. Therapeutic levels of human Factor IX[1–3,5,7], erythropoietin[8,9], and lysosomal storage enzymes[10] have been obtained in small and large animal models. When delivered into the portal vasculature, rAAV vector genomes enter almost all the hepatocytes, yet only about 5% become stably transduced regardless of cell cycle status[11]. Although the mechanism(s) underlying long-term transgene expression is not completely understood, stable rAAV genomes exist as integrated forms and/or episomal circular intermediates[12–14]. The extent to which each of these forms is responsible for stable long-term transgene expression in vivo is not known. Nevertheless, concatemers of rAAV genomes are formed concomitant with a slow rise of transgene expression following in vivo rAAV administration[12,13,15].

In the liver, rAAV vector integration into host genomes has been established by pulsed-field gel electrophoresis, fluorescent in situ hybridization (FISH), and isolation of rAAV vector–cellular DNA junctions, and these integrated proviral rAAV genomes are present as concatemers[12,13]. The formation of heteroconcatemers from two rAAV vectors has been recently demonstrated in mouse muscle and liver, and the formation of dimer intermediates by linkage of input rAAV genomes seems to be an important step for stable transduction[11,15] (Nakai et al., manuscript submitted). This suggests that co-delivery of two vectors may allow for the formation of a single functional unit and expression of one transgene through two different vectors, which will overcome the limited packaging size of current rAAV vectors.

In this study, we split a single expression cassette at an intron, producing two complementary rAAV vectors—one containing the 5′ half of the expression cassette with an enhancer/promoter and a splice donor, and the other containing the 3′ half of the cassette with a splice acceptor, a transgene, and a polyadenylation (polyA) signal. We injected these two complementary vectors into mice, to determine the relative level of gene expression compared with a single intact vector injection.

Results and discussion

Incorporation of the AAV inverted terminal repeat (ITR) sequence into an intron does not affect the correct splicing of mRNA or transgene expression. To test the feasibility of using two vectors to produce a single expression cassette and express a transgene product from a heterodimeric rAAV genome in mouse hepatocytes, we constructed different expression sequences that used the EF1αEP/nlslacZ cassette (Fig. 1A). This cassette has a 0.9 kb intron contained within the EF1αEP, which is spliced out from the final mRNA transcript. This enhancer/promoter has been shown to work efficiently in mouse liver[3]. We divided the EF1αEP/nlslacZ cassette at the *Xho*I site into two portions within the intronic sequences and identified them as EF1αEP and Pless (promoter-less)-nlslacZ cassettes (Fig. 1A). If these two portions of the expression cassette are incorporated in *cis* by heteroconcatemerization from two different rAAV constructs, reconstituting a complete EF1αEP/nlslacZ cassette, the ITR sequences would be present in the intron at the *Xho*I site of this expression cassette (see Fig. 1A).

We first used plasmid transfection assays to determine whether or not the ITR sequences within the intron would result in impaired processing of EF1αEP/nlslacZ mRNA or inefficient translation of β-galactosidase (β-gal). We constructed a plasmid, pEF1αEP-ITR-nlsLacZ, which has one ITR at the *Xho*I site in intron 1 of the *EF1*α gene, to mimic the heterodimer of two rAAV vectors reconstituting the complete EF1αEP/nlslacZ expression cassette (Fig. 1D), and

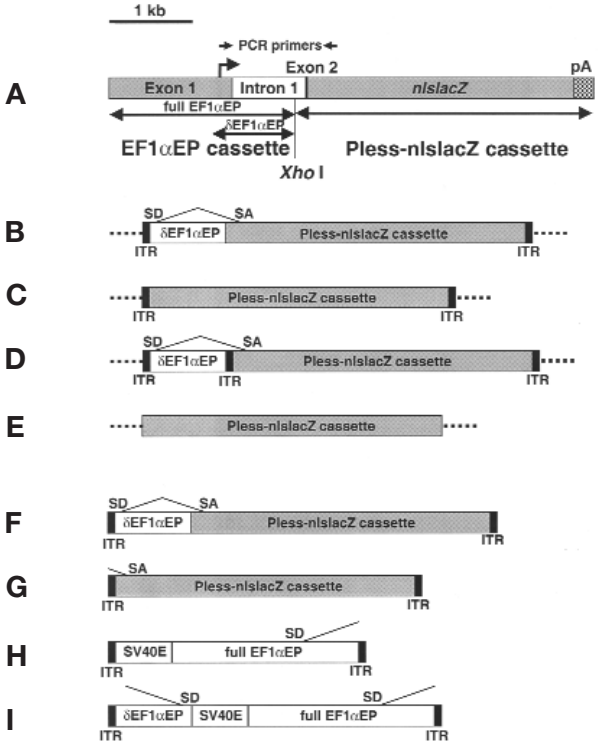

Figure 1. Structures of the EF1αEP/nlslacZ expression cassette, nlslacZ plasmids, and rAAV vectors. (A) The structure of the EF1αEP/nlslacZ cassette is shown. The EF1αEP/nlslacZ cassette comprises noncoding sequence of exons 1 and 2, and intron 1 of the *EF1α* gene, followed by the *lacZ* gene with a nuclear localizing signal (*nlslacZ*). The EF1αEP/nlslacZ cassette was divided into two portions at the *Xho*I site in the *EF1α* gene intron 1, which were defined as the EF1αEP and Pless-nlslacZ cassettes. The EF1αEP cassette has exon 1 and most of intron 1 of the *EF1α* enhancer/promoter, which includes the transcription initiation site, whereas the Pless-nlslacZ cassette has a 0.2 kb remnant of the *EF1α* enhancer/promoter, the *nlslacZ* gene, and the polyA signal. Two kinds of the EF1αEPs, full EF1αEP and δEF1αEP (ref. 12), were used for this study. The transcription initiation site is indicated by an elbow arrow, and the primer locations to amplify the EF1αEP/nlslacZ transcripts (primers, EF1αP2, and LacZP1) are shown by arrows. (B–E) Structures of the plasmids. (B) pAAV-EF1α-nlsLacZ, (C) pAAV-Pless-nlsLacZ, (D) pEF1αEP-ITR-nlsLacZ, (E) pBS-Pless-nlsLacZ. The dotted lines indicate the plasmid backbones. The splicing within the EF1αEP is shown by SD (splice donor) and SA (splice acceptor). (F–I) Structures of rAAVs. (F) AAV-EF1α-nlsLacZ, (G) AAV-Pless-nlsLacZ, (H) AAV-EF1αEP, (I) AAV-(EF1αEP)$_2$. ITR, AAV inverted terminal repeat; pA, the SV40 early polyadenylation signal; SV40E, the SV40 enhancer.

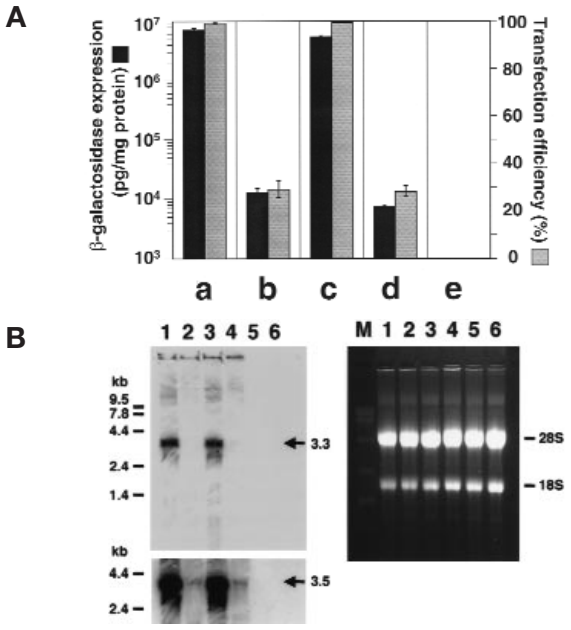

Figure 2. Transfection of 293 cells by the *nlslacZ* plasmids. (A) Transfection efficiency (gray bars) and β-gal expression (black bars) in 293 cells transfected with the *nlslacZ* plasmids. 293 cells were seeded on six-well plates at a density of 3.6 × 10^5 cells per well and transfected with 2 μg of each plasmid. The transfection efficiency and quantitation of β-gal protein were determined by Xgal staining and β-gal ELISA, respectively. The experiments were done in triplicate and the mean values are shown with error bars. The plasmids used were (a) pAAV-EF1α-nlsLacZ, (b) pAAV-Pless-nlsLacZ, (c) pEF1αEP-ITR-nlsLacZ, (d) pBS-Pless-nlsLacZ, (e) pBluescript II KS –. (B) Northern blot analysis of 293 cells transfected with *nlslacZ* plasmids. Total RNA (10 μg) was gel-separated, transferred to a nylon membrane, and hybridized with a *lacZ*/SV40 polyA probe. Lanes 1–5 represent 293 cells transfected with pAAV-EF1α-nlsLacZ, pAAV-Pless-nlsLacZ, pEF1αEP-ITR-nlsLacZ, pBS-Pless-nlsLacZ, and pBluescript II KS –, respectively. Lane 6, naïve 293 cells. The left upper panel shows a 3.3 kb EF1αEP/nlslacZ transcript. An *nlslacZ* mRNA of 3.5 kb was detected in an overexposed blot (left lower panel). Ethidium bromide-stained gel showing RNA integrity (right panel). Lane M is a 0.24–9.5 kb RNA ladder (Gibco BRL).

compared the mRNA and protein expression in vitro to that of pAAV-EF1α-nlsLacZ, pAAV-Pless-nlsLacZ, and pBS-Pless-nlsLacZ (Fig. 1B, C and E). pAAV-EF1α-nlsLacZ has a complete EF1αEP/nlslacZ expression cassette between the two ITRs; pAAV-Pless-nlsLacZ lacks the EF1αEP sequences upstream of the *Xho*I site of intron 1, but has two ITRs; pBS-Pless-nlsLacZ has the Pless-nlslacZ cassette but lacks the two ITRs. Each plasmid was transfected into 293 cells, and 36 h later β-gal expression was assessed by determining the transfection efficiency and quantity of β-gal protein (Fig. 2A). The *nlslacZ* mRNA was also analyzed by northern blot and reverse transcriptase–polymerase chain reaction (RT-PCR) (Fig. 2B and data not shown). As shown in Figure 2A and B, there was no significant difference in transgene mRNA or protein expression between pAAV-EF1α-nlsLacZ and pEF1αEP-ITR-nlsLacZ-transfected cells. The mRNA was correctly processed regardless of the presence of an ITR sequence in the intron (data not shown). When the enhancer/promoter region of EF1αEP upstream of the *Xho*I site in intron 1 was removed, producing a Pless-nlslacZ cassette, β-gal expression dropped by about 500-fold, yet there was only a 3-fold drop in the number of β-gal-positive cells (Fig. 2A). This suggested that the addition of an enhancer/promoter increased the number of transgene-specific mRNAs in each transfected cell. The low levels of β-gal protein expression from pAAV-Pless-nlsLacZ-transfected cells was presumed to come from a small amount of a second *nlslacZ* mRNA detected by northern blot analysis (Fig. 2B). The second mRNA was ~0.2 kb longer than expected from EF1αEP-driven transcripts, and was also observed in 293 cells transfected with pBS-Pless-nlsLacZ. The identity of the longer mRNA was confirmed by RT-PCR studies using different primer pairs, suggesting that the origin of the longer mRNA resulted from a cryptic transcription initiation site on the EF1αEP remnant in the Pless-nlslacZ cassette, and not from the ITR or an aberrantly spliced transcript (data not shown).

Enhancement of transgene expression from a promoter-less *nlslacZ* rAAV vector by co-injection of an enhancer/promoter rAAV vector. The ability to obtain functional mRNAs correctly spliced within an expression cassette split by an AAV-ITR allowed us to pursue a two-vector approach in vivo. We constructed a promoter-less rAAV, AAV-Pless-nlsLacZ, and two complementing vectors that contain the *EF1α* enhancer/promoter, AAV-EF1αEP and AAV-(EF1αEP)$_2$ (see Fig. 1G, H, and I). The AAV-Pless-nlsLacZ contains the 3′ remnant of the *EF1α* enhancer/promoter downstream of the

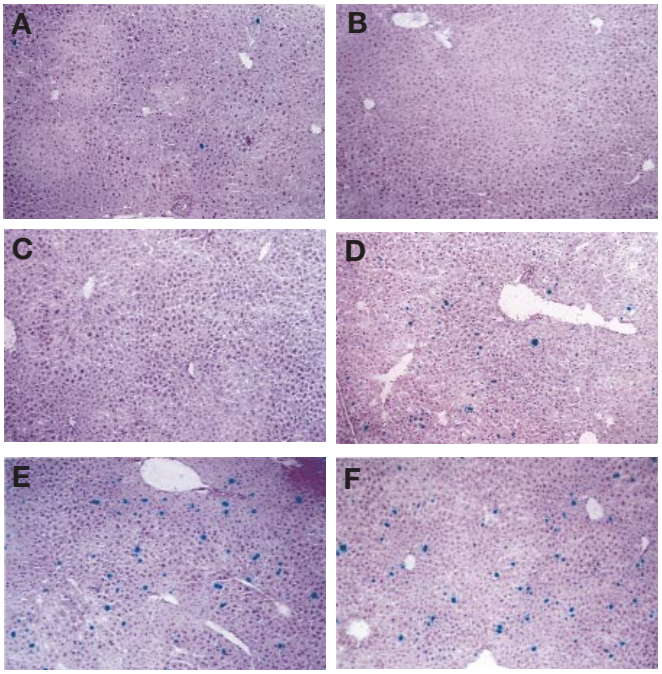

Figure 3. Xgal staining of the liver tissues from the rAAV-treated C57BL/6 rag1 mice. Six weeks after infusion via portal vein of 2.4×10^{11} particles of a single vector or of each of two vectors, the liver tissues were harvested for analysis. Shown are representative histochemical stains of liver samples from the mice injected with (A) AAV-Pless-nlsLacZ, (B) AAV-EF1αEP, (C) AAV-(EF1αEP)$_2$, (D) AAV-Pless-nlsLacZ / AAV-EF1αEP, (E) AAV-Pless-nlsLacZ / AAV- (EF1αEP)$_2$, (F) AAV-EF1α-nlsLacZ. Original magnification, 100×.

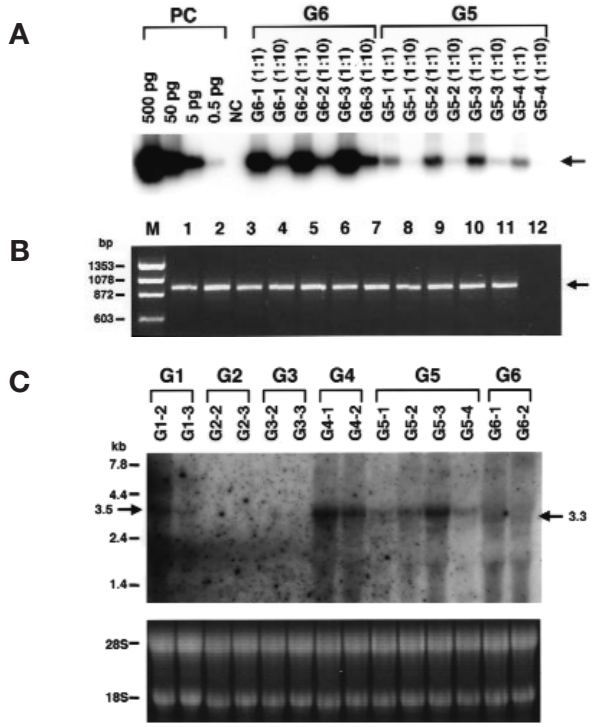

Figure 4. RNA analyses of mouse livers transduced with AAV-Pless-nlsLacZ and/or EF1αEP rAAV vector. (A) Comparison of expression of the EF1αEP/nlslacZ transcripts in transduced livers between the mice injected with AAV-EF1α-nlslacZ (group 6) and the mice co-injected with AAV-Pless-nlsLacZ and AAV-(EF1αEP)$_2$ (group 5). The data from group 4 are not shown. The EF1αEP/nlslacZ transcripts were amplified by RT-PCR using total RNA from transduced mouse livers after no dilution (1:1 dilution) or a 1:10 dilution with naïve mouse liver RNA. The PCR products were electrophoresed, transferred, and hybridized with a *lacZ* sequence-specific 30-mer oligonucleotide probe. The positive controls (PC) were pCR2.1EF1αEP/nlslacZ, and a negative control (NC) was naïve mouse liver total RNA. The groups, analyzed mice, and dilutions used are indicated above the lanes. The expected PCR fragment of 362 bp is shown by an arrow. (B) RT-PCR for murine *G3PDH* mRNA to show integrity of the RNA samples used in (A). Lanes 1–12 represent the RNA in a naïve mouse, the three mice in group 6, the four mice in group 5, the three mice in group 1, and a negative control with no RT product, respectively. The PCR products were separated on a 1.5% agarose gel and stained with ethidium bromide. The size marker (M) is ΦX174 DNA/*Hae*III digests. The expected fragment of 982 bp is indicated by an arrow. (C) Northern blot analysis of RNA from transduced mouse livers. Total RNA was separated, transferred, and hybridized with a *lacZ*/SV40 polyA probe. The experimental groups and the analyzed mice are indicated above the lanes. Faint 3.3 kb EF1αEP/nlslacZ transcripts were observed in group 6 mice, whereas 3.5 kb *nlslacZ* transcripts were detected in groups 1, 4, and 5 as indicated by the arrows. The ethidium bromide-stained gel photo is shown on the lower panel.

*Xho*I site in intron 1 (0.2 kb), the *nlslacZ* transgene, and the simian virus 40 (SV40) early polyA signal. The AAV-EF1αEP has the *EF1α* enhancer/promoter upstream of the *Xho*I site (2.2 kb) with a transcriptional orientation toward the ITR, and a fragment containing the SV40 enhancer. The AAV-(EF1αEP)$_2$ has two *EF1α* enhancer/promoters, which were placed in a head-to-head orientation with the SV40 enhancer between them. One *EF1α* enhancer/promoter was truncated by 1.3 kb (δEF1αEP[12]) because of the size limitation of rAAV packaging. Truncation of EF1αEP did not affect the enhancer/promoter activity (data not shown). A single vector, or two vectors (Fig. 1F, G, H, and I), were injected at a dose of 2.4×10^{11} particles per vector via portal vein, into six-week-old C57BL/6 rag1 mice: group 1, AAV-Pless-nlsLacZ only (n = 3); group 2, AAV-EF1αEP only (n = 3); group 3, AAV-(EF1αEP)$_2$ only (n = 3); group 4, AAV-Pless-nlsLacZ + AAV-EF1αEP (n = 2); group 5, AAV-Pless-nlsLacZ + AAV-(EF1αEP)$_2$ (n = 4); group 6, controls, AAV-EF1α-nlsLacZ (n = 3). All mice were killed six weeks after vector administration. Hepatocyte transduction efficiency was assessed by determining the proportion of Xgal-stained hepatocytes in liver sections (Fig. 3 and Table 1), and the total amount of β-gal analyzed by enzyme-linked immunosorbent assay (ELISA) from liver extracts (Table 1). Whereas the number of transduced cells gives an indication of the frequency of cells that contain heteroconcatemers, it does not estimate the total number of concatemers formed within each cell in vivo. Thus, we measured both the transduction efficiencies and total amount of transgene product when comparing each set of vectors (summarized in Table 1). No β-gal protein or transduced cells were observed in animals that received only the EF1αEP or (EF1αEP)$_2$ rAAV vectors (i.e., groups 2 and 3). Mice injected with AAV-Pless-nlsLacZ showed a low frequency of transduction at 0.5 ± 0.1% and low β-gal expression (52 ± 12 pg mg^{-1} protein), presumably due to weak promoter activity of the ITR sequences[16], or minimum promoter activity of an EF1αEP remnant[17]. When the AAV-Pless-nlsLacZ and AAV-EF1αEP vectors were co-injected, liver transduction and β-gal expression was increased to 2.9% and 236 pg mg^{-1} protein, respectively. Furthermore, when AAV-Pless-nlsLacZ was co-injected with AAV-(EF1αEP)$_2$, hepatocyte transduction and β-gal expression were restored to about 60–70% of that of the control mice injected with AAV-EF1α-nlsLacZ (4.0 ± 0.6% and 448 ± 153 pg mg^{-1} protein versus 5.8 ± 0.6% and 764 ± 221 pg mg^{-1} protein, respectively). When we compared the transduction efficiency and β-gal expression between the three mice injected with the promoter-less vector (group 1), and the six mice co-injected with the promoter-less and an enhancer/promoter vector (groups 4 and 5), a Mann–Whitney U-test revealed a statistically significant difference ($p < 0.025$). The amount of β-gal protein in transduced livers measured by β-gal ELISA paralleled the transduction efficiencies or the number of the Xgal-positive hepatocytes

Table 1. Efficiency of hepatocyte transduction and β-galactosidase expression in mouse hepatocytes following rAAV administration[a]

	Transduction efficiency[b] (%) and β-galactosidase expression[c] (pg mg^{-1} protein)					Relative transduction[d]
	Mouse				Mean ± s.d.	
	1	2	3	4		
G1: AAV-Pless-nlsLacZ	0.5 (47)	0.6 (68)	0.3 (40)	–	0.5 ± 0.1 (52 ± 12)	0.09 (0.07)
G2: AAV-EF1aEP	0.0 (<1)	0.0 (<1)	0.0 (<1)	–	0.0 (<1)	N/A
G3: AAV-(EF1aEP)$_2$	0.0 (<1)	0.0 (<1)	0.0 (<1)	–	0.0 (<1)	N/A
G4: AAV-Pless-nlsLacZ AAV-EF1aEP	2.8 (263)	2.9 (208)	–	–	2.9 (236)	0.50 (0.31)
G5: AAV-Pless-nlsLacZ AAV-(EF1aEP)$_2$	5.0 (246)	3.9 (676)	3.9 (419)	3.2 (450)	4.0 ± 0.6 (448 ± 153)	0.69 (0.59)
G6: AAV-EF1a-nlsLacZ	5.2 (1,072)	5.6 (564)	6.6 (656)	–	5.8 ± 0.6 (764 ± 221)	1.00 (1.00)

[a]G1–G6, groups 1–6 (see text); N/A, not applicable.
[b]Xgal-positive nuclei / total nuclei counted (%).
[c]β-galactosidase antigen levels in liver extracts were normalized by total protein in samples (pg mg-1 protein), and shown in parentheses.
[d]Relative transduction efficiency and β-galactosidase expression (shown in parentheses) as compared to group 6 (G6).

(Table 1). These observations demonstrate that transgene expression in liver from a promoter-less rAAV vector can be significantly enhanced by a second vector with an enhancer/promoter, reaching as high as 60–70% of the levels of that obtainable by a single, complete rAAV expression cassette.

The mechanism of the enhanced gene expression from two vectors. Recent studies have demonstrated that heteroconcatemers are formed in mouse hepatocytes after intraportal administration of two rAAV vectors[11] (Nakai et al., manuscript submitted), hence we reasoned that a heterodimer consisting of AAV-Pless-LacZ and EF1αEP rAAV should reconstitute the complete EF1αEP/nlslacZ expression cassette, allowing for correct transcription and mRNA processing, and ultimately β-gal gene expression in mouse hepatocytes. To demonstrate this, total RNA was extracted from the transduced mouse livers, and EF1αEP/nlslacZ transcripts were analyzed by RT-PCR. Similar to the studies performed in cultured cells, the PCR primers were designed to detect mRNA transcripts that originated from the proper transcriptional initiation site. EF1αEP/nlslacZ mRNA transcripts were not detected in liver from animals injected with AAV-Pless-nlsLacZ only (group 1), whereas the expected RT-PCR fragments were observed in the livers of mice co-injected with AAV-Pless-nlsLacZ and AAV-EF1αEP (group 4) (data not shown). Even greater amounts of the *cis*-spliced mRNAs were found when AAV-(EF1αEP)$_2$ was used in place of AAV-EF1αEP (group 5) (Fig. 4A and B). This suggests that a single expression cassette divided into two rAAV vectors can be reconstituted by intermolecular ligation, and mRNA can be correctly processed if the vectors are designed to have the ITR sequences between the vectors spliced out from the mRNA.

However, as determined by the RT-PCR analysis, the relative increase in the expected *cis*-spliced mRNA in mice that were co-injected with two vectors was not sufficient by itself to explain the restoration of β-gal protein expression (Fig. 4A and B). The restoration of β-gal protein expression was higher than expected based on a statistical calculation of the probability for two rAAV vectors to link in a correct orientation. If dimer formation and linking orientation are random events, the probability for a dimer to be a heterodimer in a correct orientation allowing for *cis*-splicing would be one eighth, when AAV-EF1αEP and AAV-Pless-nlsLacZ were co-delivered (group 4). Similarly the maximum restoration of expression from AAV-(EF1αEP)$_2$ that contained an enhancer/promoter in two orientations would be one fourth (group 5). This suggests that the β-gal restoration by *cis*-spliced mRNA should have been at most 13% and 25% in groups 4 and 5, respectively, compared to that of the complete single vector (group 6). To answer this question, we performed northern blot analyses. Similarly to what was found in the tissue culture studies, in mice that received two vectors, there were two *nlslacZ* mRNA transcripts that varied in size by about 0.2 kb. The predominant species in the AAV-EF1α-nlsLacZ vector-injected mice was the 3.3 kb transcript, whereas in the mice treated with AAV-Pless-nlsLacZ, there was only a 3.5 kb mRNA transcript (Fig. 4C). The hepatic expression of this larger *nlslacZ* mRNA from AAV-Pless-nlsLacZ was further enhanced when mice were co-injected with an enhancer/promoter vector (Fig. 4C). Taken together, enhancement of transgene expression in mice injected with two vectors was the result of both the expected *cis*-spliced EF1αEP/nlsLacZ mRNA transcribed from a heterodimer and presumably orientation-independent *cis*-enhancer activity of the EF1αEP(s) to the *nlslacZ* mRNA transcription in the Pless-nlslacZ cassette by EF1αEP vectors. The model explaining the presumed mechanism(s) for enhanced gene expression is summarized in Figure 5.

In a previous study, we mixed two vectors and performed two-color-probe FISH analysis, demonstrating that stable rAAV heteroconcatemers were present in about 40% of the hepatocytes containing stable vector genomes[11]. While this method did not measure the number of hepatocytes that were able to express two transgene products, the 40% value was close to the 50–70% relative efficiency of transduction detected by restoration of β-gal expression using two split vectors, compared to one complete vector. Some of the quantitative variations may also be due to differences in the detection limits using FISH and Xgal staining. Further studies into the mechanism of rAAV transduction are required to fully sort out these differences.

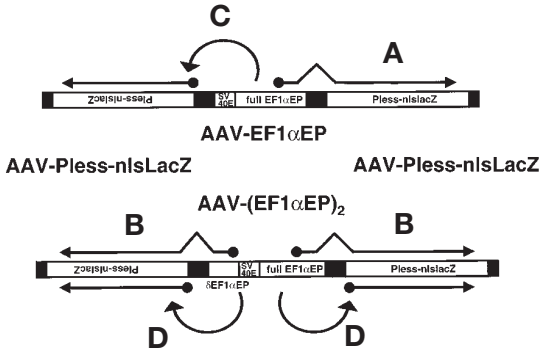

Figure 5. Possible mechanisms of in vivo enhancement of transgene expression from AAV-Pless-nlsLacZ vector by AAV-EF1αEP or AAV-(EF1αEP)$_2$ vector. (A) Unidirectional transcription from the *EF1α* enhancer/promoter in an AAV-EF1αEP / AAV-Pless-nlsLacZ heterodimer. (B) Bidirectional transcription from AAV-(EF1αEP)$_2$ in an AAV-Pless-nlsLacZ / AAV-(EF1αEP)$_2$ / AAV-Pless-nlsLacZ heterotrimer. (C) Orientation-independent *cis*-enhancement of the larger, 3.5 kb *nlslacZ* mRNA expression by AAV-EF1αEP. (D) *Cis*-enhancement of the larger *nlslacZ* mRNA by AAV-(EF1αEP)$_2$. Because the vector sequences flanking the ITRs are frequently deleted[12], *cis*-splicing may not necessarily occur in an AAV-(EF1αEP)$_2$ / AAV-Pless-nlsLacZ heterodimer. In this case, AAV-(EF1αEP)$_2$ may work as a *cis*-enhancer of the larger *nlslacZ* mRNA. The black boxes indicate the ITRs.

Biological applications. Previous to this study, expression of functional proteins in individual cells from two rAAV vectors have been demonstrated in vivo to enhance a biological pathway[18] or to control transgene expression[9]. More recently, Burton et al. successfully expressed a single functional protein, the human coagulation Factor VIII, in mouse liver by co-injection of two rAAV vectors, which expressed two peptide chains that associated into a functional single protein before secretion[19]. This approach would overcome the size limitation of rAAV packaging, but is applicable only for a limited number of proteins. In addition, the uncoupled proteins may have detrimental effects depending on their biological function.

The demonstration of *cis*-splicing from two complementary rAAV vectors in hepatocytes is of great importance, because it suggests that a large cDNA can be expressed by this novel rAAV vector approach. In addition, the demonstration of *cis* enhancement of a slightly larger mRNA, transcribed from a cryptic transcription start site in a single rAAV by a second enhancer/promoter vector, suggests that greater enhancement would be achievable if we incorporated an efficient promoter upstream of a cDNA in a rAAV vector and co-delivered it with a second vector, where only the *cis*-enhancement effect of the second enhancer vector would occur. In this case, the minimal promoter sequence without an enhancer could be used, and a relatively large cDNA could be incorporated in a single vector.

A two-rAAV-vector system based on the recently elucidated molecular structure of rAAV concatemers may greatly increase the usefulness of rAAV vectors. The expression of the *cystic fibrosis transmembrane conductance regulator* (*CFTR*) gene, which has been hampered by the inefficient promoter activity of the ITR[16], could be enhanced to achieve a therapeutic level of gene expression by a second vector, and the *human coagulation Factor VIII* gene, both of whose cDNAs barely fit into an rAAV vector, could be combined with a large tissue-specific enhancer/promoter contained in a second vector. Insertional mutagenesis is always a consideration with an integrating vector. Whether a rAAV vector containing only regulatory elements has more risk of activating a detrimental silent gene than a vector with a complete expression cassette, should be carefully addressed for the clinical applications of this strategy. Further elucidation of the mechanism of rAAV transduction and integration could address this safety issue and might lead us to other novel approaches to enhance hepatocyte transduction, which is currently limited to approximately 5% of total hepatocytes.

Experimental protocol

Construction of rAAV vectors and plasmids. All of the recombinant AAV vectors we used in this study were constructed based on AAV type 2. AAV-EF1α-nlsLacZ, AAV-Pless-nlsLacZ, AAV-EF1αEP, and AAV-$(EF1\alpha EP)_2$ vectors were produced based on the following vector plasmids: pAAV-EF1α-nlsLacZ, pAAV-Pless-nlsLacZ, pAAV-EF1αEP, and pAAV-$(EF1\alpha EP)_2$, respectively. To construct pAAV-EF1α-nlsLacZ, an nls was taken from HR2PGKnlslacZ[20] and incorporated into the 5′ end of the cytoplasmic *lacZ* gene of pAAV-EF1α-LacZ[11]. pAAV-Pless-nlsLacZ was produced by removing a 0.9 kb 5′ portion of the δEF1αEP[12] including the TATA box, transcription initiation site, the splice donor of exon 1, and most of intron 1, leaving a 0.2 kb 3′ end of the *EF1α*-noncoding sequence including intron 1 and the splice acceptor of exon 2 of the *EF1α* gene.

The two enhancer/promoter rAAV vector plasmids, pAAV-EF1αEP and pAAV-$(EF1\alpha EP)_2$ were constructed as follows. The human Factor IX cDNA, polyA signal, and 0.2 kb 3′ end of the *EF1α* enhancer/promoter downstream of the *Xho*I site in intron 1, were removed from pV4.1e-hF.IX (ref. 3). A 2.1 kb *EF1α* enhancer/promoter sequence upstream of the *Xho*I site in intron 1 was left between the two ITRs, making pITR-EF1αEP-ITR. A *Xba*I-*Hin*cII-*Bam*HI linker was inserted into pITR-EF1αEP-ITR at the 5′ end of the EF1α enhancer/promoter to make pITR-XHB-EF1αEP-ITR. A fragment of pASNori2 (ref. 21) containing the SV40 enhancer was subcloned into a pBluescript II KS– (Stratagene, La Jolla, CA)-based cloning plasmid, and the *Bam*HI/*Bgl*II fragment containing the transferred SV40 sequences was inserted into the unique *Bam*HI site upstream of the *EF1α* enhancer/promoter, making pITR-XH-SV40E-EF1αEP-ITR or pAAV-EF1αEP. A 0.9 kb *Xba*I/*Xho*I fragment of δEF1αEP was excised from pAAV-EF1α-LacZ, blunted, and then inserted into a unique *Hin*cII site of pITR-XH-SV40E-EF1αEP-ITR, in a head-to-head orientation relative to the other *EF1α* enhancer/promoter, producing pITR-δEF1αEP-SV40E-EF1αEP-ITR or pAAV-$(EF1\alpha EP)_2$.

pEF1αEP-ITR-nlsLacZ was constructed as follows. A 2.3 kb *Xba*I/*Sse* 8387I fragment of pITR-EF1αEP-ITR, containing the EF1αEP and 3′-ITR, was ligated to a 6.6 kb *Xho*I/*Xba*I fragment of pAAV-EF1α-LacZ, containing a 0.2 kb EF1αEP remnant downstream of the *Xho*I site in *EF1α* gene intron 1, the *lacZ* gene, SV40 polyA, 3′-ITR, and 5′-ITR, to make pEF1αEP-ITR-LacZ. This pEF1αEP-ITR-LacZ has an EF1αEP/cytoplasmic *lacZ* expression cassette with an ITR at the *Xho*I site in intron 1 of the *EF1α* gene, between two ITRs. The entire δEF1αEP of pAAV-EF1α-nlsLacZ was replaced with a δEF1αEP containing an ITR in the intron 1 of pEF1αEP-ITR-LacZ, to make pEF1αEP-ITR-nlsLacZ. pBS-Pless-nlsLacZ was constructed by insertion of a *Not*I/*Not*I fragment of pAAV-Pless-nlsLacZ containing the whole Pless-nlslacZ cassette without ITRs, into a unique *Not*I site of pBluescript II KS –.

All the rAAV vectors were prepared using the adenovirus-free triple-plasmid transfection method[22] with pHLP19 (ref. 19), an AAV helper plasmid that has been shown to make no recombinant wild-type AAV particles at a sensitively of 1 functional AAV virion in a background of 10^9 rAAV particles. The vector purification procedure was outlined elsewhere[19]. The physical vector titer was determined by a quantitative dot blot assay[8].

In vitro transfection of 293 cells with rAAV plasmids. We maintained 293 cells in Dulbecco's modified Eagle medium (DMEM; Gibco BRL, Gaithersburg, MD) supplemented with 10% fetal bovine serum (FBS; Hyclone, Logan, UT) and penicillin-streptomycin (Gibco BRL), and seeded on six-well plates at a density of 3.6×10^5 cells per well. After 24 h, 293 cells were transfected with 2 μg of each plasmid by calcium phosphate method[23]. The cells were harvested 36 h after transfection for RNA and protein extraction. For Xgal staining, cells were trypsinized 32 h after transfection and reseeded onto new six-well plates with 5% of the total cells. The transfection efficiency was determined by Xgal staining 36 h after the addition of DNA. The protein analysis and Xgal staining were done in triplicate.

Animal procedures. Six-week-old male C57BL/6 rag1 mice were obtained from Jackson Laboratory. All animal experiments were performed according to the guidelines for animal care at Stanford University. The animals were anesthetized by inhalation of methoxyflurane (Metofane, Mallinckrodt Veterinary Inc., Mundelein, IL), and 200 μl of rAAV vector preparations were infused into the portal vein as described[3]. All mice were killed six weeks post-injection, and liver samples were collected for protein, RNA, and histological analyses.

Histological analysis. A piece from each four major liver lobes was embedded in Tissue-Tek O.C.T. compound (Sakura Finetek USA, Inc., Torrence, CA), and frozen on dry ice. Frozen sections (10 μm) were prepared, stained with Xgal as described[24], and counterstained with hematoxylin. Approximately 500 hepatocyte nuclei were counted from each lobe, with more than 2,000 nuclei counted in total for each mouse. The hepatocyte transduction efficiency was calculated by dividing the number of Xgal-positive nuclei by the total number of nuclei counted. Photomicroscopy was performed with Eclipse E800 (Nikon, Melville, NY).

Protein analysis. Expression levels of β-gal in transfected 293 cells and transduced mouse livers were determined by ELISA using a β-Gal ELISA Kit (Roche Molecular Biochemicals, Indianapolis, IN). Briefly, total protein was extracted from transfected 293 cells according to the manufacturer's recommendation, and extraction of cytoplasmic and nuclear protein from mouse livers was performed as described by Gorski et al. with a modification[25]. Total protein concentration in samples was measured based on the Lowry assay[26] using a DC Protein Assay kit (Bio-Rad, Hercules, CA) with bovine serum albumin as a standard. The results of β-gal ELISA were normalized with the total protein concentration.

RNA analysis of the liver samples. Frozen mouse liver tissue (100–150 mg) was placed directly into 1.5 ml of RNA STAT-60 reagent (Tel-Test "B", Friendswood, TX) and homogenized with a motor-driven disposable plastic pestle. Total RNA was extracted according to the manufacturer's recommendation. For RT-PCR, total RNA was treated with DNase I (DNase I, amplification grade, Gibco BRL) at a concentration of 1 unit μg^{-1} total RNA at room temperature for 15 min, then incubated at 65°C for 10 min in the presence of 2.3 mM EDTA to inactivate DNase I, and quickly chilled on ice. The RT reaction was performed using a First-Strand cDNA Synthesis Kit (Amersham Pharmacia, Piscataway, NJ) with random hexamers, and cDNA corresponding to 0.3 μg total RNA was used for the subsequent RT-PCR to amplify the

EF1αEP/nlslacZ mRNA and murine *glyceraldehyde 3-phosphate dehydrogenase* (*G3PDH*) mRNA. The primers used for RT-PCR are given below.

EF1α P2: 5′-CTTTTTCGCAACGGGTTTGCCGCCAGAACACA-3′
LacZ P1: 5′-GACAGTATCGGCCTCAGGAAGA-3′
mG3PDH P1: 5′-CAGTGGCAAAGTGGAGATTGTT-3′
mG3PDH P2: 5′-TACTCCTTGGAGGCCATGTAGG-3′

RT-PCR was carried out in the 50 μl PCR mixture containing 10 mM Tris HCl (pH 8.3), 50 mM KCl, 1.5 mM $MgCl_2$, 200 μM of each deoxynucleoside triphosphate, 0.4 μM each primer, and 2.5 units of *Taq* DNA polymerase. The PCR cycle conditions were 95°C for 2 min, followed by 30 cycles of 95°C for 1 min, 58°C for 30 s, and 72°C for 30 s for the amplification of EF1αEP/nlslacZ mRNA, and 95°C for 2 min, followed by 30 cycles of 95°C for 1 min, 60°C for 1 min, and 72°C for 1 min for amplification of murine *G3PDH* mRNA. A 10–20 μl aliquot of each PCR reaction mixture was separated on a 1.5% agarose gel, and the bands were visualized with ethidium bromide staining. The EF1αEP/nlslacZ RT-PCR products were then transferred to a Duralon UV membrane (Stratagene, La Jolla, CA) and hybridized with a ^{32}P-labeled *lacZ*-specific oligonucleotide probe, 5′-CGGGAATTCACTGGCCGTCGTTTTACAACG-3′. The signals were detected by a Molecular Imager System (BioRad, Hercules, CA). The positive control plasmid for EF1αEP/nlslacZ RT-PCR, pCR2.1EF1αEP/nlslacZ, was constructed by inserting the RT-PCR product into plasmid pCR2.1, using an Original TA Cloning Kit (Invitrogen, Carlsbad, CA). RT-PCR positive controls were generated as follows. A known amount of pCR2.1EF1αEP/nlslacZ (i.e., 500, 50, 5, and 0.5 pg) was added into a RT-PCR reaction mixture containing RT product from 0.3 μg of total RNA from naïve mouse liver, and PCR cycles were carried out as described. Some RNA samples were subjected to RT-PCR after dilution with total RNA from naïve mouse liver to keep the total amount of RNA per tube constant.

Northern blot analysis was performed according to Sambrook and colleagues[27] using 10 μg of total RNA from 293 cells, or 20 μg of total RNA from mouse liver. Total RNA was denatured, separated on a 1.0% formaldehyde gel, transferred to a Duralon UV membrane, hybridized with a ^{32}P-labeled 2.3 kb-*lacZ*/SV40 polyA probe, and autoradiographed at -80°C.

Acknowledgment

We thank Sally Fuess for technical assistance. This work was supported by NIH ROI HL53682.

1. Herzog, R.W. et al. Stable gene transfer and expression of human blood coagulation factor IX after intramuscular injection of recombinant adeno-associated virus. *Proc. Natl. Acad. Sci. USA* **94**, 5804–5809 (1997).
2. Herzog, R.W. et al. Long-term correction of canine hemophilia B by gene transfer of blood coagulation factor IX mediated by adeno-associated viral vector. *Nat. Med.* **5**, 56–63 (1999).
3. Nakai, H. et al. Adeno-associated viral vector-mediated gene transfer of human blood coagulation factor IX into mouse liver. *Blood* **91**, 4600–4607 (1998).
4. Russell, D. & Kay, M.A. rAAV and hematology. *Blood* **94**, 864–874 (1999).
5. Snyder, R.O. et al. Persistent and therapeutic concentrations of human factor IX in mice after hepatic gene transfer of recombinant AAV vectors. *Nat. Genet.* **16**, 270–276 (1997).
6. Snyder, R.O. et al. Efficient and stable adeno-associated virus-mediated transduction in the skeletal muscle of adult immunocompetent mice. *Hum. Gene Ther.* **8**, 1891–1900 (1997).
7. Snyder, R.O. et al. Correction of hemophilia B in canine and murine models using recombinant adeno-associated viral vectors. *Nat. Med.* **5**, 64–70 (1999).
8. Kessler, P.D. et al. Gene delivery to skeletal muscle results in sustained expression and systemic delivery of a therapeutic protein. *Proc. Natl. Acad. Sci. USA* **93**, 14082–14087 (1996).
9. Rendahl, K.G. et al. Regulation of gene expression in vivo following transduction by two separate rAAV vectors. *Nat. Biotechnol.* **16**, 757–761 (1998).
10. Watson, G.L. et al. Treatment of lysosomal storage disease in MPS VII mice using a recombinant adeno-associated virus. *Gene Ther.* **5**, 1642–1649 (1998).
11. Miao, C.H. et al. Non-random transduction of recombinant adeno-associated viral vectors in mouse hepatocytes in vivo: cell cycling does not influence hepatocyte transduction. *J. Virol.* **74**, 3793–3803 (2000).
12. Nakai, H., Iwaki, Y., Kay, M.A. & Couto, L.B. Isolation of recombinant adeno-associated virus vector–cellular DNA junctions from mouse liver. *J. Virol.* **73**, 5438–5447 (1999).
13. Miao, C.H. et al. The kinetics of rAAV integration in the liver. *Nat. Genet.* **19**, 13–15 (1998).
14. Duan, D. et al. Circular intermediates of recombinant adeno-associated virus have defined structural characteristics responsible for long-term episomal persistence in muscle tissue. *J. Virol.* **72**, 8568–8577 (1998).
15. Yang, J. et al. Concatamerization of adeno-associated virus circular genomes occurs through intermolecular recombination. *J. Virol.* **73**, 9468–9477 (1999).
16. Flotte, T.R. et al. Expression of the cystic fibrosis transmembrane conductance regulator from a novel adeno-associated virus promoter. *J. Biol. Chem.* **268**, 3781–3790 (1993).
17. Kim, D.W., Uetsuki, T., Kaziro, Y., Yamaguchi, N. & Sugano, S. Use of the human elongation factor 1α promoter as a versatile and efficient expression system. *Gene* **91**, 217–223 (1990).
18. Fan, D.S. et al. Behavioral recovery in 6-hydroxydopamine-lesioned rats by cotransduction of striatum with tyrosine hydroxylase and aromatic L-amino acid decarboxylase genes using two separate adeno-associated virus vectors. *Hum. Gene Ther.* **9**, 2527–2535 (1998).
19. Burton, M. et al. Coexpression of factor VIII heavy and light chain adeno-associated viral vectors produces biologically active protein. *Proc. Natl. Acad. Sci. USA* **96**, 12725–12730 (1999).
20. Naldini, L. et al. In vivo gene delivery and stable transduction of nondividing cells by a lentiviral vector. *Science* **272**, 263–267 (1996).
21. Russell, D.W. & Hirata, R.K. Human gene targeting by viral vectors. *Nat. Genet.* **18**, 325–330 (1998).
22. Matsushita, T. et al. Adeno-associated virus vectors can be efficiently produced without helper virus. *Gene Ther.* **5**, 938–945 (1998).
23. Wigler, M. et al. Transformation of mammalian cells with an amplifiable dominant-acting gene. *Proc. Natl. Acad. Sci. USA* **77**, 3567–3570 (1980).
24. Kay, M.A. et al. Hepatic gene therapy: persistent expression of human α1- antitrypsin in mice after direct gene delivery in vivo. *Hum. Gene Ther.* **3**, 641–647 (1992).
25. Gorski, K., Carneiro, M. & Schibler, U. Tissue-specific in vitro transcription from the mouse albumin promoter. *Cell* **47**, 767–776 (1986).
26. Lowry, O.H., Rosebrough, N.J., Farr, A.L. & Randall, R.J. Protein measurement with the folin phenol reagent. *J. Biol. Chem.* **193**, 265–275 (1951).
27. Sambrook, J., Fritsch, E.F. & Maniatis, T. *Molecular cloning: a laboratory manual*, Edn. 2 (Cold Spring Harbor Laboratory Press, Cold Spring Harbor, NY; 1989).